SIAM J. NUMER. ANAL.
Vol. 35, No. 6, pp. 2169–2194, December 1998

004

NONCLASSICAL SHOCKS AND KINETIC RELATIONS: FINITE DIFFERENCE SCHEMES*

BRIAN T. HAYES† AND PHILIPPE G. LEFLOCH‡

This paper is dedicated to the memory of Ami Harten, who, along with coinvestigators Mac Hyman and Peter Lax, was among the avant garde in the study of entropy-violating shocks in numerical schemes.

Abstract. We consider hyperbolic systems of conservation laws that are not genuinely nonlinear. The solutions generated by diffusive-dispersive regularizations may include nonclassical (n.c.) shock waves that do not satisfy the classical Liu entropy criterion. We investigate the numerical approximation of n.c. shocks via conservative difference schemes constrained only by a *single entropy inequality.* The schemes are designed by comparing their equivalent equations with the continuous model and include discretizations of the diffusive and dispersive terms.

Limits of these schemes are characterized via the *kinetic relation* introduced earlier by the authors. We determine the kinetic function numerically for several examples of systems and schemes. This study demonstrates that the kinetic relation is a suitable tool for the selection of unique n.c. solutions and for the study of their *sensitive dependence* on the critical parameters: the ratios of diffusion/dispersion and diffusion/mesh size, the shock strength, and the order of discretization of the flux.

Key words. hyperbolic conservation laws, diffusion, dispersion, shock wave, undercompressive, entropy inequality

AMS subject classifications. 35L65, 65M60

PII. S0036142997315998

1. Introduction.

This paper is part of a series devoted to systems of conservation laws and to the notion of weak solutions not satisfying the classical entropy conditions [10, 11]. The focus is on strictly hyperbolic systems admitting one or more characteristic fields which are *not* genuinely nonlinear. We recall that solutions to nonlinear hyperbolic equations are generally discontinuous and cannot be uniquely determined from their initial data. Classically, one attempts to single out the physically relevant solutions by the so-called *entropy criterion*.

For nongenuinely nonlinear systems, the Liu criterion leads to the classical entropy solutions, as we call them. For the Riemann problem, Liu's construction [24] provides a unique solution that depends continuously upon its end states.

Shock waves violating the Liu criterion do arise, however, as limits of diffusive-dispersive regularizations of hyperbolic systems. This happens when the system is not genuinely nonlinear, and the diffusion and the dispersion are kept in *balance.* Many models in continuum mechanics fall into this category: nonlinear elastodynamics, magnetohydrodynamics, dynamics of complex fluids, etc. Dispersive effects have various physical sources: capillarity effects in viscous fluids, the Hall effect in magnetic fluids, etc. In the models arising in concrete applications, both the lack of genuine nonlinearity and the coexistence of diffusive and dispersive effects are often realized.

*Received by the editors January 31, 1997; accepted for publication (in revised form) September 2, 1997; published electronically November 13, 1998.

http://www.siam.org/journals/sinum/35-6/31599.html

†Department of Mathematics, Duke University, Durham, NC 27708 (hayes@math.duke.edu).

‡Centre de Mathématiques Appliquées and Centre National de la Recherche Scientifique, UA 756, Ecole Polytechnique, 91128 Palaiseau Cedex, France (lefloch@cmapx.polytechnique.fr). This author was partially supported by CNRS, NSF grants DMS 94-01003 and DMS 95-02766 and a Faculty Early Career Development (CAREER) award, and by AFOSR grant F49620-94–1-0215.

At the core of this work is an observation Lax built on in his early mathematical studies of shock wave solutions to systems of conservation laws [18, 19]. Every system arising in physics can be endowed with one strictly convex entropy function. For smooth solutions, this provides us with an additional conservation law; for discontinuous solutions, one can develop a selection criterion in the form of an *entropy inequality.* The Lax inequality is *independent* of the underlying regularization, i.e., independent of the physical constants such as the capillarity, viscosity, or other parameters.

This latter property demonstrates both the power and the limitation of the Lax entropy inequality. On one hand, the Lax–Wendroff theorem [20], for instance, implies that, for genuinely nonlinear and strictly hyperbolic systems, any entropy consistent, conservative scheme can converge only toward the physically relevant solutions. On the other hand, in the presence of "small-scale dependent" solutions, the whole strategy appears to fail.

The existence of shock waves sensitive to regularization has been long recognized, but in rather different contexts (e.g., nonstrictly hyperbolic systems, hyperbolic-elliptic systems, nonconservative systems) from the one we emphasize in this study. (See [11] for a list of references.) We focus on a somewhat limited class of problems (shocks with small strength to strictly hyperbolic and nongenuinely nonlinear systems), with the aim of developing a practical tool for studying the existence, uniqueness, and properties of the nonclassical shocks generated by balanced diffusive-dispersive effects. In [11], we observed that precisely one entropy inequality, in general, can be derived for limiting solutions of a class of diffusive-dispersive approximations.

Building on work by Abeyaratne and Knowles [1, 2], Truskinovsky [31, 32], and LeFloch [21], we developed in [10, 11] the concept of a kinetic relation, which provides a selection principle for the nonclassical shocks and therefore, jointly with the entropy inequality, plays the role the latter performs alone for genuinely nonlinear systems.

The Riemann problem in this class was studied in Hayes and LeFloch [11]: it admits a multiparameter family of entropy solutions. Under generic assumptions, each nongenuinely nonlinear characteristic field generates a *two-dimensional wave set* instead of the classical one-dimensional wave curve. The Riemann problem can then be solved *uniquely* with classical waves and nonclassical shocks, provided we stipulate that the entropy dissipation across any nonclassical shock is a given, constitutive function. For certain systems, the entropy dissipation may be expressed as a function of the propagation speed of the n.c. shock. We call such an admissibility criterion a *kinetic relation*. We use the term *admissible nonclassical entropy solution* for a solution of a nongenuinely nonlinear system that satisfies an entropy inequality together with a kinetic relation.

The present paper addresses the issue of numerical computation of nonclassical shocks. A main challenge for the theory lies in developing shock-capturing techniques adapted to n.c. shocks. One of the difficulties is that the Lax–Wendroff theorem is no longer sufficient to design adapted shock capturing schemes: it merely ensures that the limiting solutions satisfy one entropy inequality, while this inequality alone does not guarantee uniqueness for nongenuinely nonlinear systems.

One approach is to attempt to resolve the small-scale structure of the shocks; this is out of reach in a number of concrete applications. Another approach is to track the n.c. fronts in the solutions [4, 33], a task which becomes rather complicated when fronts interact, especially in multidimensional problems. A strategy that bypasses some of the difficulties is to keep track of the location of the n.c. shocks via a level set formulation [14].

Studies on numerical schemes for computing solutions of a hyperbolic-elliptic phase transition model, utilizing the viscosity-capillarity regularization, have been undertaken by Slemrod and Flaherty [28], Affouf and Caflisch [3], Cockburn and Gau [5], Jin [16], and Shu [27], among others.

In section 2 of this paper, we study a class of difference schemes which fit into the general framework of [11]. We consider a continuous model containing vanishing diffusive-dispersive terms and attempt to numerically compute the *limiting solutions* generated by the continuous model without resolving the small-scale structures. To this end a family of discrete models is proposed, which are conservative and consistent and satisfy a local, *discrete entropy inequality*. We deal here with general systems of conservation laws, hyperbolic or not, regularized with diffusion and dispersion terms that are *linear* functions of the *entropy variable,* i.e., the gradient of the entropy with respect to the conservative variable. The schemes under consideration are based on a suitable discretization of the diffusive-dispersive terms of the continuous model. Several specific schemes are investigated for the cases of the system of elastodynamics and the scalar conservation law with cubic flux. The latter is the prototype of a nongenuinely nonlinear equation, and in this case, by applying the method of compensated compactness, we show the strong convergence of a class of schemes.

From experiments with difference schemes for nongenuinely nonlinear systems, it turns out [10] that certain schemes produce classical solutions while others give nonclassical ones. Our goal in section 3 is to derive conditions ensuring or excluding the generation of n.c. shocks.

For scalar equations, the condition that the scheme does not increase the total variation (i.e., satisfies the famous TVD criterion introduced by Harten [8]) guarantees that all limiting solutions will be classical.

In section 3 we study three types of schemes, corresponding to different discretizations of the hyperbolic flux function: a first-order approximation based on the Lax–Friedrichs or upwinding schemes; a second-order, entropy conservative approximation (after Tadmor [30]); and a higher-order approximation designed to closely mimic the continuous equation.

For each scheme, we derive an *equivalent equation* based on a Taylor expansion in the mesh size. This equation is compared with the original, continuous model and used as a *preliminary* indicator as to whether the limiting solutions of the continuous and discrete models approach each other. Based on the sign of the dispersive term of the equivalent equation, we determine a threshold in the shock strength below which the solutions are classical. The use of the equivalent equation is not rigorous for solutions containing shocks, but heuristically is expected to be accurate for shocks having small strength (Goodman and Majda [7], Hou and LeFloch [13]).

At first glance, numerical results for all of the schemes under study seem to produce the same nonclassical shocks. The equivalent equation was also used to design nonconservative schemes [17] and in phase dynamics [5].

In section 4, we study the limitations of the approach based on the equivalent equation. We demonstrate that the kinetic function is a useful tool for the analysis of nonclassical shocks. We display first the kinetic function in the state variables, i.e., the right state of an n.c. shock versus its left state. These curves are independent of the entropy under consideration. From these graphs we calculate the kinetic functions directly from the entropy dissipation and the jump conditions.

By numerically computing the (distinct) kinetic functions for several specific schemes, we observe the sensitive dependence upon the parameters such as the ratio

of diffusion to dispersion and the ratio of diffusion to mesh size. The former is to be expected from the analysis of the continuous model, but the latter is atypical.

Three regimes in the shock strength are distinguished: for weak shocks and fixed diffusion/dispersion ratio, the kinetic functions are indistinguishable from the (continuous) traveling wave solution. Beyond this, there is always some discrepancy. In an intermediate range of shock strength, the higher-order approximation almost matches the (continuous) traveling wave solution. For strong shocks, none of the numerical methods can reproduce the kinetics of the continuous model.

In some applications, it may desirable to prevent the formation of nonclassical shocks, as when no specific physical effects are sought. The equivalent equation could then be used as a tool to select the classical solution. An empirical requirement is that the dispersion coefficient have a certain sign. It would be interesting to find rigorous criteria.

In [9], Harten, Hyman, and Lax demonstrate that the Lax–Wendroff scheme converges to an entropy-violating solution for the scalar conservation law with flux $f(u) = u - \alpha u^2(1-u)^2, \alpha > 0$. They write, presciently, that "It seems that both the non-monotonicity of the finite-difference scheme and the non-convexity of the flux function are responsible for this non-physical behavior of the solution." The present work aims at a deeper understanding of just how the nonlinearity of the flux and the high-order nature of the numerical scheme interact to produce a certain type of entropy-violating shocks.[1]

2. Entropy stability.

2.1. General systems.

Consider a system of conservation laws:

$$u_t + f(u)_x = 0, \qquad u(x,t) \in \mathbb{R}^p, \quad x \in \mathbb{R}, \quad t > 0, \tag{2.1}$$

endowed with an entropy-entropy flux pair $(U, F) : \mathbb{R}^p \to \mathbb{R}^2$, i.e., a pair of functions satisfying the compatibility condition $\nabla_u F = \nabla_u U \cdot D_u f$. Here $f : \mathbb{R}^p \to \mathbb{R}^p$ is a smooth mapping, called the flux-function of (2.1). We are interested in weak solutions to (2.1) satisfying the entropy inequality:

$$U(u)_t + F(u)_x \leq 0. \tag{2.2}$$

The main focus is on systems that are strictly hyperbolic but not genuinely nonlinear. The discussion in this subsection and in 2.2 also applies to *mixed* (hyperbolic-elliptic) systems. In both cases the Riemann problem for (2.1)–(2.2) does not, in general, possess a unique solution.

The entropy inequality (2.2) is generally the only such inequality which is valid for a class of approximations to (2.1). Our purpose in this section is to consider a class of schemes which approximate (2.1) and satisfy a discrete version of (2.2). The schemes will explicitly contain both diffusive and dispersive effects, in balance. Such an entropy consistency is essential but does not select a unique solution. In the following sections of this paper we will search for additional constraints induced by the approximations on the limiting solutions.

Consider for a moment the case where U is strictly convex, so that (2.1) is hyperbolic and can be symmetrized via the change of variable $v := \hat{v}(u) := \nabla U(u)$, called the entropy variable. The mapping $u \to v$ is one-to-one and system (2.1) becomes

$$\tilde{u}(v)_t + \tilde{f}(v)_x = 0, \tag{2.3}$$

[1] These shocks, however, do not fit directly in our framework since they do not satisfy an entropy inequality of the form (2.2).

where $\tilde{u}(v) := u$ and $\tilde{f}(v) := f(u)$. Also define $\tilde{U}(v) := U(u), \dots$. Using the compatibility condition, which implies that $\nabla_u^2 U \cdot D_u f$ is a symmetric matrix, we see that the matrices $D_v \tilde{u}(v)$ and $D_v \tilde{f}(v)$ are symmetric.

Considering the symmetric formulation (2.3) of (2.1), we introduce the following regularization which adds diffusion and dispersion:

$$\tilde{u}(v^\epsilon)_t + \tilde{f}(v^\epsilon)_x = \epsilon\, v^\epsilon_{xx} + \alpha\, \epsilon^2\, v^\epsilon_{xxx}. \tag{2.4}$$

Here α is a real parameter measuring the ratio of the dispersion to the diffusion terms, and ϵ is a small positive parameter. The limiting function $v := \lim_{\epsilon \to 0} v^\epsilon$ (if the limit exists in a strong sense) is a solution of (2.3). Furthermore, upon multiplying (2.4) by v^ϵ, we observe that the left-hand side takes the conservative form $\tilde{U}(v^\epsilon)_t + \tilde{F}(v^\epsilon)_x$, while, on the right-hand side, the diffusion yields a *conservative* term plus a *dissipative* one,

$$\epsilon\, v^\epsilon \cdot v^\epsilon_{xx} = \epsilon \left(\frac{|v^\epsilon|}{2} \right)_{xx} - \epsilon \left| v^\epsilon_x \right|^2,$$

and the dispersion is *entropy conservative*:

$$\alpha\, \epsilon^2 v^\epsilon \cdot v^\epsilon_{xxx} = \alpha\, \epsilon^2 \Big(v^\epsilon \cdot v^\epsilon_{xx} - \frac{|v^\epsilon_x|^2}{2} \Big)_x.$$

(We denote by a dot and $|.|$ the scalar product and the norm in $\mathbb{R}^p$.) Under suitable conditions on the convergence of v^ϵ as $\epsilon \to 0$, it follows that v^ϵ satisfies

$$\int_{\mathbb{R}} \tilde{U}(v^\epsilon(T))\, dx + \epsilon \int_0^T \int_{\mathbb{R}} \left| v^\epsilon_x \right|^2 dxdt = \int_{\mathbb{R}} \tilde{U}(v^\epsilon(0))\, dx, \qquad T \geq 0, \tag{2.5}$$

and the limit v satisfies

$$\tilde{U}(v)_t + \tilde{F}(v)_x \leq 0, \tag{2.6}$$

which is nothing but the entropy inequality (2.2), provided a function u is defined from v by the formula $u = \big(\nabla_u U\big)^{-1}(v)$.

At this stage of the discussion, we note that the entire analysis also applies *without* assuming U to be convex, as was observed by Levermore [23]. Consider system (2.1) regularized as follows:

$$u^\epsilon_t + f(u^\epsilon)_x = \epsilon\, \hat{v}(u^\epsilon)_{xx} + \alpha\, \epsilon^2\, \hat{v}(u^\epsilon)_{xxx}. \tag{2.7}$$

Similarly, as in the derivation of (2.5), (2.6), we can check that u^ϵ satisfies

$$\int_{\mathbb{R}} U(u^\epsilon(T))\, dx + \epsilon \int_0^T \int_{\mathbb{R}} \left| \hat{v}(u^\epsilon)_x \right|^2 dxdt = \int_{\mathbb{R}} U(u^\epsilon(0))\, dx, \tag{2.8}$$

and that the limit $u := \lim_{\epsilon \to 0} u^\epsilon$ satisfies the conservation law (2.1) and the entropy inequality (2.2). Observe again that the diffusion $\epsilon\, \hat{v}(u^\epsilon)_{xx}$ is dissipative for the entropy U while the dispersion $\alpha\, \epsilon^2\, \hat{v}(u^\epsilon)_{xxx}$ is entropy conservative. For additional material and rigorous proofs involving the vanishing diffusion-dispersion limit for nongenuinely nonlinear problems, we refer to [6, 10, 11, 22, 25].

We now extend the above analysis to a class of schemes which approximate (2.7).

Denote by $u_j(t)$ an approximation to $u(x_j,t)$, where the points $x_j := j\,h$ describe a mesh of length $h \to 0$. To obtain a continuous in time scheme, there are three terms to be discretized in (2.7). The discretization of the term $f(u)_x$ is based on a conservative $(2\,k+1)$-point numerical flux,

$$g^0 : \mathbb{R}^{2k+1} \to \mathbb{R}, \quad g^0(u,u,\dots,u) := f(u) \qquad \text{for all } u. \tag{2.9}$$

For the diffusion and dispersion, we use high-order accurate, centered finite differences. The accuracy of the discretization is a central issue to be discussed in section 3, while the present section aims at deriving a discrete entropy inequality.

Specifically, we introduce the following conservative, continuous in time, discrete in space, difference scheme:

$$\frac{d}{dt}u_j(t) + \frac{1}{h}\big(g_{j+1/2}(t) - g_{j-1/2}(t)\big) = 0, \qquad t \geq 0, \tag{2.10i}$$

where

$$g_{j+1/2} := g^0_{j+1/2} + g^1_{j+1/2} + g^2_{j+1/2}, \tag{2.10ii}$$

$$g^0_{j+1/2} := g^0(u_{j-k+1}, u_{j-k+2}, \dots, u_{j+k}),$$

$$g^1_{j+1/2} := -\frac{\beta}{2}\left(\hat v(u_{j+1}) - \hat v(u_j)\right),$$

$$g^2_{j+1/2} := -\frac{\gamma}{6}\Big(\hat v(u_{j+2}) - \hat v(u_{j+1}) - \hat v(u_j) + \hat v(u_{j-1})\Big). \tag{2.10iii}$$

The initial data are discretized in a standard fashion. In (2.10) the parameters $\beta > 0$ and $\gamma \in \mathbb{R}$ are *fixed* but should be thought of as

$$\beta\,h := \kappa_1\,\epsilon, \qquad \gamma\,h^2 := \kappa_2\,\alpha\,\epsilon^2, \tag{2.11}$$

with precise constants κ_1 and κ_2 given later in section 3 by deriving the equivalent equation of the scheme. One anticipates that, under certain assumptions, the $h \to 0$ *limit* of (2.10) should be a good approximation to the $\epsilon \to 0$ *limit* of (2.7). However, the scheme (2.10) is also studied here for its own sake. Note that the scheme naturally balances the effects of diffusion and dispersion.

Our basic requirement in arriving at (2.10) from (2.7) was the following: the discrete problem should satisfy, as does the continuous problem, an entropy inequality of the form

$$\frac{d}{dt}U\big(u_j(t)\big) + \frac{1}{h}\big(G_{j+1/2}(t) - G_{j-1/2}(t)\big) \leq 0, \qquad t \geq 0, \tag{2.12}$$

where $G_{j+1/2} := G(u_{j-m+1}, u_{j-m+2}, \dots, u_{j+m})$ and $G : \mathbb{R}^{2m+1} \to \mathbb{R}$ (the numerical entropy flux) is consistent with the exact entropy flux, i.e., $G(u,u,\dots,u) := F(u)$ for all u. When (2.12) holds, we say that the scheme (or the numerical flux) is *entropy dissipative*. Following Tadmor [29, 30], we say that a scheme is *entropy conservative* when (2.12) holds as an equality for all j.

Indeed, our proposed discretization of the diffusion and dispersion allows us to retain the entropy inequality of the continuous model.

THEOREM 2.1. *Consider an entropy pair (U,F) for the system* (2.1). *Suppose that when $\beta = \gamma = 0$, the scheme* (2.10) *satisfies a local entropy inequality with*

numerical entropy flux G^0. *Then, for all* $\beta \geq 0$ *and* γ, *the scheme* (2.10) *satisfies the local, discrete entropy inequality* (2.12) *with*

$$
\begin{aligned}
G_{j+1/2} &:= G^0_{j+1/2} + G^1_{j+1/2} + G^2_{j+1/2},\\
G^1_{j+1/2} &:= -\frac{\beta}{2}\,\hat{v}(u_j)\Big(\hat{v}(u_{j+1}) - \hat{v}(u_j)\Big),\\
G^2_{j+1/2} &:= -\frac{\gamma}{6}\Big(\hat{v}(u_{j+2})\,\hat{v}(u_j) + \hat{v}(u_{j+1})\,\hat{v}(u_{j-1}) - 2\,\hat{v}(u_{j+1})\,\hat{v}(u_j)\Big).
\end{aligned}
\tag{2.13}
$$

When the scheme is L^∞ *stable and convergent almost everywhere* (*a.e.*) *as* $h \to 0$, *the limiting function is a single entropy solution, i.e., satisfying* (2.1), (2.2). ∎

The entropy inequality (2.2) satisfied at the limit is *independent* of the parameters β and γ. It is therefore too lax to characterize a unique solution to the Riemann problem, since we shall check in section 4 that the solutions generated by the scheme (2.10) *do depend* on β and γ in general.

Observe that the entropy U need *not* be convex in Theorem 2.1. Our result applies when, for instance, the flux term $f(u)_x$ is discretized with an entropy conservative, numerical flux g^0. (This choice has definite advantages, as we will see in section 3.)

Proof of Theorem 2.1. Multiplying both sides of (2.10i) by $\tilde{v}(u_j)$, we arrive at the following identity:

$$
h\,\frac{d}{dt}U(u_j(t)) + G_{j+1/2}(t) - G_{j-1/2}(t) = -D^0_j(t) - D^1_j(t) \leq 0, \qquad t \geq 0,
\tag{2.14}
$$

where $G_{j+1/2}$ is given by (2.13) and

$$
\begin{aligned}
D^0_j &:= \hat{v}(u_j)\big(g^0_{j+1/2} - g^0_{j-1/2}\big) - G^0_{j+1/2} + G^0_{j-1/2},\\
D^1_j &:= \frac{\beta}{2}\,\big|\hat{v}(u_j) - \hat{v}(u_{j-1})\big|^2.
\end{aligned}
\tag{2.15}
$$

Observe that $D^0_j(t) \geq 0$ since g^0 is entropy dissipative, while obviously $D^1_j(t) \geq 0$ when $\beta \geq 0$.

The Lax–Wendroff theorem [20] may be applied to obtain the second part of the theorem. ∎

By summation in j and integration in t of (2.14), we arrive at the uniform entropy estimate:

$$
\sum_{j\in\mathbf{Z}} U(u_j(T))\,h + \sum_{j\in\mathbf{Z}} \int_0^T \big(D^0_j(t) + D^1_j(t)\big)\,dt = \sum_{j\in\mathbf{Z}} U(u_j(0))\,h,
\tag{2.16}
$$

which is a discrete version of the entropy stability (2.8).

2.2. Elastodynamics model. Consider the system of two conservation laws:

$$
\begin{aligned}
v_t - \sigma(w)_x &= \epsilon\, v_{xx} - \alpha\,\epsilon^2\, w_{xxx},\\
w_t - v_x &= 0,
\end{aligned}
\tag{2.17}
$$

where $v(x,t)$ and $w(x,t)$ are the velocity and the deformation gradient of a material at the point (x,t), respectively. The stress-law $w \to \sigma(w)$ is a function depending on the material under consideration. For definiteness we treat the case

$$
\sigma(w) = w^3 + a\,w,
\tag{2.18}
$$

with a being a real parameter.

Consider system (2.17) with $\epsilon = 0$. When $a > 0$, it is strictly hyperbolic and admits two real and distinct wave speeds, $\pm c(w) := \pm\sqrt{3\,w^2 + a}$; when $a = 0$, it is strictly hyperbolic except on the line $\{w = 0\}$; when $a < 0$, it is strictly hyperbolic in the range $\{3\,w^2 > |a|\}$ but elliptic in $\{3\,w^2 < |a|\}$.

Theorem 2.1 could be applied (with the choice of entropy (2.19) given below) provided that the dispersion term w_{xxx} in (2.17) were replaced with $\big(\sigma(w)\big)_{xxx}$, which is an entropy conservative regularization. The dispersion w_{xxx} is not entropy conservative, and Theorem 2.1 needs to be extended.

Observe first that the model (2.17) actually *dissipates* the entropy

$$U(v,w) = \frac{w^4}{4} + \frac{v^2 + a\,w^2}{2}, \qquad F(v,w) := -v\,\big(w^3 + a\,w\big). \tag{2.19}$$

Namely we have

$$\Big(U(v,w) + \alpha\,\epsilon^2\,\frac{w_x^2}{2}\Big)_t + \Big(F(v,w)\Big)_x = \epsilon\,\big(v\,v_x\big)_x - \epsilon\,v_x^2 - \alpha\,\epsilon^2\,\big(-v\,w_{xx} + w_t\,w_{xx}\big)_x.$$

So if the convergence $(v_\epsilon, w^\epsilon) \to (v,w)$ is strong and $\epsilon^2\,w_x^2 \to 0$ (which is known when $a > 0$; cf. [11]), we recover the inequality

$$\Big(\frac{v^2}{2} + \frac{w^4}{4} + a\,\frac{w^2}{2}\Big)_t - \Big(v\,(w^3 + a\,w)\Big)_x \leq 0. \tag{2.20}$$

Note that the entropy in (2.19) is strictly convex iff $a > 0$.

Fix initial data $(\bar v, \bar w)$ for the hyperbolic problem, i.e., (2.17) with $\epsilon = 0$. Discretize (2.17)–(2.18), in a similar spirit to (2.10), but now using an entropy conservative flux for $\sigma(w)_x$ and v_x. Given β and γ, we propose the following scheme:

$$(v_j(0), w_j(0)) = \frac{1}{h}\int_{x_{j-1/2}}^{x_{j+1/2}} (\bar v(y), \bar w(y))\,dy \tag{2.21}$$

and

$$\begin{aligned} &\frac{d}{dt}v_j(t) + \frac{1}{h}\big(g^v_{j+1/2}(t) - g^v_{j-1/2}(t)\big) = 0, \qquad t \geq 0,\\ &\frac{d}{dt}w_j(t) + \frac{1}{h}\big(g^w_{j+1/2}(t) - g^w_{j-1/2}(t)\big) = 0, \qquad t \geq 0, \end{aligned} \tag{2.22i}$$

where

(2.22ii)
$$g^v_{j+1/2} := g^{v,0}_{j+1/2} + g^{v,1}_{j+1/2} + g^{v,2}_{j+1/2}, \qquad g^w_{j+1/2} := g^{w,0}_{j+1/2} + g^{w,1}_{j+1/2} + g^{w,2}_{j+1/2},$$

$$\begin{aligned} g^{v,0}_{j+1/2} &:= -\big(w^3_{j+1} + w^3_j + a\,w_{j+1} + a\,w_j\big)/2, \qquad g^{w,0}_{j+1/2} := -(v_{j+1} + v_j)/2,\\ g^{v,1}_{j+1/2} &:= -\frac{\beta}{2}\,(v_{j+1} - v_j), \qquad g^{w,1}_{j+1/2} := 0,\\ g^{v,2}_{j+1/2} &:= \frac{\gamma}{6}\,\Big(w_{j+2} - w_{j+1} - w_j + w_{j-1}\Big), \qquad g^{w,2}_{j+1/2} := 0. \end{aligned} \tag{2.22iii}$$

THEOREM 2.2. *For all $\beta \ge 0$ and all reals a and γ, the scheme* (2.21)–(2.22) *satisfies the discrete entropy inequality*

(2.23)
$$\frac{1}{2}\frac{d}{dt}\Big(v_j^2 + \frac{w_j^4}{4} + a\,w_j^2 + \gamma\,(w_{j+1}-w_j)^2\Big) + \frac{1}{h}\big(G_{j+1/2}(t) - G_{j-1/2}(t)\big) \le 0, \quad t \ge 0,$$

where $G_{j+1/2} := G^0_{j+1/2} + G^1_{j+1/2} + G^2_{j+1/2}$,

$$\begin{aligned}
G^0_{j+1/2} &:= -(1/2)\,\big(v_j\,\sigma(w_{j+1}) + v_{j+1}\,\sigma(w_j)\big),\\
G^1_{j+1/2} &:= -\frac{\beta}{2}\,v_j\,\big(v_{j+1}-v_j\big),\\
G^2_{j+1/2} &:= \frac{\gamma}{6}\,\big(v_j w_{j+2} - v_j w_{j+1} - 2v_{j+1}w_j - v_{j+2}w_{j+1}\\
&\qquad + v_{j+2}w_j + v_{j+1}w_{j-1} + v_{j+1}w_{j+1}\big).
\end{aligned} \tag{2.24}$$

When $a, \beta, \gamma > 0$, the scheme satisfies the following uniform bounds:

(2.25)
$$\sum_j \Big(v_j(t)^2 + w_j(t)^4 + a\,w_j(t)^2 + \gamma\,(w_{j+1}-w_j)^2\Big) \le C\,\big(\|\bar v\|^2_{L^2} + \|\bar w\|^2_{L^2} + \|\bar w\|^4_{L^4}\big). \quad \square$$

Proof of Theorem 2.2. Multiply the equations in (2.22i) by v_j and $\sigma(v_j)$, respectively:

$$\begin{aligned}
&h\,\frac{d}{dt}\Big(\frac{v_j^2}{2} + \frac{w_j^4}{4} + a\,\frac{w_j^2}{2}\Big) + v_j\,\big(g^{v,0}_{j+1/2} - g^{v,0}_{j-1/2}\big) + \sigma(w_j)\,\big(g^{w,0}_{j+1/2} - g^{w,0}_{j-1/2}\big)\\
&+ v_j\,\big(g^{v,1}_{j+1/2} - g^{v,1}_{j-1/2}\big) + v_j\,\big(g^{v,2}_{j+1/2} - g^{v,2}_{j-1/2}\big) = 0.
\end{aligned}$$

First of all we have

$$\begin{aligned}
&v_j\,\big(g^{v,0}_{j+1/2} - g^{v,0}_{j-1/2}\big) + \sigma(w_j)\,\big(g^{w,0}_{j+1/2} - g^{w,0}_{j-1/2}\big)\\
&= -\frac{1}{2}\Big(v_j\,\big(\sigma(v_{j+1}) - \sigma(v_{j-1})\big) + \sigma(v_j)\,\big(v_{j+1} - v_{j-1}\big)\Big)\\
&= G^0_{j+1/2} - G^0_{j-1/2}.
\end{aligned}$$

Next we have

$$v_j\,\big(g^{v,1}_{j+1/2} - g^{v,1}_{j-1/2}\big) = G^1_{j+1/2} - G^1_{j-1/2} + D^1_j,$$

where $D^1_j := (\beta/2)\,|v_j - v_{j-1}|^2 \ge 0$.

Finally we treat the third term:

$$v_j\,\big(g^{v,2}_{j+1/2} - g^{v,2}_{j-1/2}\big) = G^2_{j+1/2} - G^2_{j-1/2} + (v_{j+2}-v_j)(w_{j+1}-w_j) - (v_{j+1}-v_{j-1})(w_{j+1}-w_j).$$

We now use the second equation from (2.22i), at the $(j+1)$st and the jth gridpoints, to eliminate v from the last two terms in the above line. We obtain

$$v_j\big(g^{v,2}_{j+1/2} - g^{v,2}_{j-1/2}\big) = G^2_{j+1/2} - G^2_{j-1/2} + \frac{h}{2}\,\frac{d}{dt}(w_{j+1}-w_j)^2,$$

and the entropy inequality (2.23) then follows from combining the contributions from the three terms in the flux decomposition.

The uniform bound (2.25) is then obtained by summing (2.23) over j and integrating from 0 to t in time. ∎

In view of the estimate (2.25), the convergence theorem established in [11] for the continuous model (2.17) easily extends to the scheme (2.22), allowing us to prove that it converges strongly to a weak solution satisfying the entropy inequality (2.20). Bounds like (2.25) were obtained by Cockburn and Gau [5] for a scheme (different from ours) approximating (2.17) with a piecewise linear stress function.

2.3. Cubic conservation law. Consider the Cauchy problem for the scalar conservation law with cubic flux $f(u) := u^3$, that is,

$$\partial_t u + \partial_x u^3 = 0, \tag{2.26}$$

$$u(x,0) = \bar{u}(x), \qquad x \in \mathbb{R}, \tag{2.27}$$

where $\bar{u}$ is given. Solutions of (2.26) that are limits of u_ϵ given by

$$\partial_t u_\epsilon + \partial_x u_\epsilon^3 = \epsilon\, \partial_{xx} u_\epsilon + \alpha\, \epsilon^2\, \partial_{xxx} u_\epsilon \tag{2.28}$$

are sought. Such solutions satisfy the entropy inequality

$$\partial_t \left(\frac{u^2}{2} \right) + \partial_x \left(\frac{3\, u^4}{4} \right) \leq 0. \tag{2.29}$$

Observe that the characteristic speed $f'(u) := 3\, u^2$ is positive for $u \neq 0$.

Given $\beta > 0$ and $\gamma \in \mathbb{R}$, we introduce the scheme

$$\frac{d}{dt} u_j(t) + \frac{1}{h} \big(g_{j+1/2}(t) - g_{j-1/2}(t) \big) = 0, \tag{2.30i}$$

(2.30ii)

$$g_{j+1/2} := g^0_{j+1/2} + g^1_{j+1/2} + g^2_{j+1/2}, \qquad g^0_{j+1/2} := u_j^3,$$

$$g^1_{j+1/2} := -\frac{\beta}{4} \left(u_{j+2} + u_{j+1} - u_j - u_{j-1} \right), \quad g^2_{j+1/2} := -\frac{\gamma}{6} \left(u_{j+2} - u_{j+1} - u_j + u_{j-1} \right).$$

We also set

$$u_j(0) = \frac{1}{h} \int_{x_{j-1/2}}^{x_{j+1/2}} \bar{u}(y)\, dy. \tag{2.31}$$

A family of piecewise constant, approximate solutions $u^h(x,t)$ is defined from the $u_j(t)$'s by $u(x,t) = u_j(t)$ if $x \in \big[x_{j-1/2}, x_{j+1/2} \big)$.

Observe that Theorem 2.1 applies to scheme (2.30), since u itself is the entropy variable associated with the entropy $U(u) = u^2/2$ and the upwinding scheme used for g^0 is entropy dissipative. However, the result of Theorem 2.1 can be improved in the scalar case: it is a remarkable property of the discrete model (2.30)–(2.31) that it preserves an *additional invariant* of the continuous problem, closely related to the entropy $u^4/4$ of the hyperbolic equation. This is the key for us in establishing a strong convergence result.

THEOREM 2.3. *Consider the Cauchy problem* (2.26)–(2.27) *with* $\bar{u} \in L^1(\mathbb{R}) \cap L^4(\mathbb{R})$. *For all* $\beta \geq 0$ *and* γ, *the scheme* (2.30)–(2.31) *satisfies the discrete entropy inequality* (2.12) *with* $U(u) = u^2/2$, $G_{j+1/2} := G^0_{j+1/2} + G^1_{j+1/2} + G^2_{j+1/2}$, *and*

$$
\begin{aligned}
G^0_{j+1/2} &:= (3/4)\, u_j^4, \\
G^1_{j+1/2} &:= -\frac{\beta}{4}\big(u_{j+2}^2 - u_{j+2}\, u_j + u_{j+1}^2 - u_{j+1}\, u_{j-1}\big), \\
G^2_{j+1/2} &:= -\frac{\gamma}{6}\,\big(u_{j+2}\, u_j + u_{j+1}\, u_{j-1} - 2\, u_{j+1}\, u_j\big).
\end{aligned} \tag{2.32}
$$

The scheme is stable in $L^\infty\big((0,T), L^1(\mathbb{R}) \cap L^4(\mathbb{R})\big)$ *for every* $T > 0$. *As* $h \to 0$, *(a subsequence of)* u^h *converges strongly in* $L^q\big((0,T), L^p(\mathbb{R})\big)$, *for all* $q \in [1,\infty)$, $p \in [1,4)$, *and* $T > 0$, *to a weak solution* u *of the Cauchy problem* (2.26)–(2.27). ∎

Remark. 1) The entropy inequality (2.29) formally follows from the discrete entropy inequality obtained in Theorem 2.3. However, it cannot be rigorously derived with the estimates currently available, since u need not be in $L^\infty_{\text{loc}}(L^4)$, and thus the entropy flux may not be a function but merely a measure.

2) When $\gamma \neq 0$, the schemes are not TVD. As a matter of fact, it follows from the analysis in [10] that at least for piecewise smooth, limiting solutions, a TVD scheme that is consistent with (at least) one entropy inequality can only converge to a classical entropy solution. This is so because, for a range of initial data, nonclassical shocks do increase the total variation of the initial data. (See Figure 3.1b in next section.) ∎

Proof of Theorem 2.3. Proceeding as in the proof of Theorem 2.1, we obtain the following entropy balance for the entropy $U(u) = u^2/2$:

$$
\begin{aligned}
&(h/2)\,\frac{d}{dt} u_j^2 + G_{j+1/2} - G_{j-1/2} \\
&\quad = -(1/4)\,\big(u_j^2 + 2\, u_j\, u_{j-1} + 3\, u_{j-1}^2\big)\big(u_j - u_{j-1}\big)^2 - (\beta/4)\,\big(u_{j+1} - u_j\big)^2,
\end{aligned} \tag{2.33}
$$

where we use the notation (2.32). In particular this provides the uniform bound

$$
h \sum_j u_j^2(t) + \sum_j \int_0^T \big(\beta + u_j^2(t) + u_{j-1}^2(t)\big)\,\big(u_j(t) - u_{j-1}(t)\big)^2\, dt \leq C\, \|\bar{u}\|_{L^2}. \tag{2.34}
$$

To obtain higher-order bounds, we estimate the entropy production/dissipation associated with $u^4/4$. Multiply (2.30i) by u_j^3, sum over j, and integrate by parts to obtain

$$
\begin{aligned}
(h/4)\,\frac{d}{dt}\sum_j u_j^4 &+ (1/2)\,\sum_j \big(u_j^2 + u_j\, u_{j-1} + u_{j-1}^2\big)^2\,\big(u_j - u_{j-1}\big)^2 \\
&+ (\beta/4)\,\sum_j \big(u_j^2 + u_j\, u_{j+2} + u_{j+2}^2\big)^2\,\big(u_{j+2} - u_j\big)^2 \\
&- (\gamma/6)\,\sum_j u_j^3\,\big(u_{j+2} - 2\, u_{j+1} + 2\, u_{j-1} - u_{j-2}\big) = 0.
\end{aligned} \tag{2.35}
$$

All of the terms in (2.35) have a favorable sign, except the term containing γ.

Next consider (2.30) with j replaced by $j \pm 1$, respectively, and subtract the two corresponding formulas. Multiply by the difference $u_{j+1} - u_{j-1}$. After integrating by parts, we get

$$
\begin{aligned}
&(h/2)\,\frac{d}{dt}\sum_j \big(u_{j+1}-u_{j-1}\big)^2 \\
&+\sum_j u_j^3\,\big(u_{j+2}-2\,u_{j+1}+2\,u_{j-1}-u_{j-2}\big)+(\beta/4)\,\sum_j \big(u_{j+2}-2\,u_j+u_{j-2}\big)^2 \\
&-(\gamma/6)\,\sum_j \big(u_{j+1}-u_{j-1}-u_{j-3}+u_{j+1}\big)\,\big(u_{j+3}-2\,u_{j+2}+2\,u_j-u_{j-1}\big)=0.
\end{aligned}
\tag{2.36}
$$

Two remarkable properties of (2.35) and (2.36) are to be noted. The "bad term" found in (2.35) arises once more as the second term in (2.36), and actually with a different sign, which allows us to eliminate it by summation of the two identities. On the other hand the last sum in (2.36) is found to be zero, by integrating by parts several times. We therefore obtain

(2.37)
$$
\begin{aligned}
&h\,\frac{d}{dt}\sum_j\left(\frac{u_j^4}{4}+\frac{\gamma}{12}\big(u_{j+1}-u_{j-1}\big)^2\right)+(1/2)\,\sum_j\big(u_j^2+u_j\,u_{j-1}+u_{j-1}^2\big)^2\,\big(u_j-u_{j-1}\big)^2 \\
&+\frac{\beta\,\gamma}{24}\sum_j\big(u_{j+2}-2\,u_j+u_{j-2}\big)^2+\frac{\beta}{4}\sum_j\big(u_{j+1}^2+u_{j+1}\,u_{j-1}+u_{j-1}^2\big)\big(u_{j+1}-u_{j-1}\big)^2=0.
\end{aligned}
$$

The following uniform bounds have been derived:

(2.38)
$$
\sum_j\Big(u_j^4(t)+u_j^2(t)+\gamma\,\big(u_{j+1}(t)-u_{j-1}(t)\big)^2\Big)\,h\le C\,\big(\|\bar u\|_{L^4}^4+\|\bar u\|_{L^2}^2\big),\qquad t\ge 0,
$$

(2.39)
$$
\begin{aligned}
&\sum_j\int_0^T\big(\beta+u_{j+1}^4+u_j^4+u_{j+1}^2+u_j^2\big)\,dt+\beta\sum_j\int_0^T\big(u_{j+1}^2+u_{j-1}^2\big)\,\big(u_{j+1}(t)-u_{j-1}(t)\big)^2\,dt \\
&+\beta\,\gamma\,\sum_j\big(u_{j+2}-2\,u_j+u_{j-2}\big)^2\,dt\le C\,\big(\|\bar u\|_{L^4}^4+\|\bar u\|_{L^2}^2\big).
\end{aligned}
$$

These are discrete analogues of the estimates obtained in [10] for the continuous problem. In view of (2.38)–(2.39), a proof based on the method of compensated compactness follows in a standard fashion. (See Schonbek [25] and Hayes and LeFloch [10].) This yields the strong convergence in L^p for $p \in [1, 4)$. □

3. Equivalent equation. In this section we present a hierarchy of difference schemes approximating the continuous problem, (2.1)–(2.2), based on how accurately the flux term is discretized. To fix ideas, we focus on the following choices:

Scheme I: First-order, entropy dissipative discretization of the flux.

Scheme II: Second-order, entropy conservative discretization.

Scheme III: Fourth-order discretization.

As long as the solution involves only classical shocks, the single entropy inequality derived in section 2 is sufficient to guarantee uniqueness of the weak solutions (at least in the class of the piecewise smooth solutions and for the Riemann problem, which is the primary concern in this paper). This means that all schemes would converge to the same solution, in that case. In the present discussion we study the case where the entropy inequality does not determine the limiting solutions, and different schemes may converge to distinct limits.

For each scheme we consider its equivalent equation. We attempt to predict heuristically whether or not nonclassical shocks will arise for that scheme. To this end, the sign of the dispersion coefficient appears to be crucial. It would be desirable to use a third (or higher) order entropy conservative discretization of the flux function. However, it can be checked (Hayes and LeFloch [12]) that no such numerical flux exists.

3.1. Cubic conservation law. For all three choices of numerical flux, the scheme is assumed to have the form

(3.1)
$$\frac{du_j}{dt} + \frac{g^0_{j+1/2} - g^0_{j-1/2}}{h} = \frac{\beta}{2h}\big(u_{j+1} - 2\,u_j + u_{j-1}\big) + \frac{\gamma}{6h}\big(u_{j+2} - 2\,u_{j+1} + 2\,u_{j-1} - u_{j-2}\big),$$

where $g^0_{j+1/2}$ is a discrete flux consistent with u^3.

We want to compare the equivalent equations corresponding to the three choices of numerical flux with (2.28). Since (2.28) is consistent with the entropy inequality (2.29), we expect that numerical schemes whose equivalent equations also satisfy (2.29) to better approximate the limiting solutions generated by the vanishing approximation (2.28). We recall [15, 10] that for the continuous problem (2.28), nonclassical behavior is observed *only when* $\alpha > 0$.

Scheme I. Upwinding scheme with numerical flux:

$$g^0_{j+1/2} = (u_j)^3. \tag{3.2}$$

The equivalent equation for (3.1) in this case is

$$u_t + (u^3)_x = h\left(u^3/2 + \beta\,u/2\right)_{xx} + h^2\left(\gamma\,u/3 - u^3/6\right)_{xxx} + O(h^3). \tag{3.3}$$

The flux contribution to the dispersive term, $u^3/6$, occurs with the opposite sign, compared to the γ-term. We therefore expect a competition between the linear term, tending to produce nonclassical shocks, and the cubic term, tending to prevent nonclassical shocks. For sufficiently strong shocks, it might be anticipated that (with γ fixed) the cubic, i.e., classical, behavior would win out. Note that due to the presence of both u_{xxx} and $(u^3)_{xxx}$, neither of the entropies $u^2/2$ or $u^4/4$ are dissipated by the equivalent equation (3.3).

Scheme II. Entropy conservative flux:

$$g^0_{j+1/2} = \frac{1}{4}\frac{(u_{j+1})^4 - (u_j)^4}{u_{j+1} - u_j}, \tag{3.4}$$

which leads to the equivalent equation

$$u_t + (u^3)_x = h\,\frac{\beta}{2}u_{xx} + \frac{h^2}{2}\left(\frac{2\,\gamma}{3}u_{xx} - u^2 u_{xx} - u(u_x)^2\right)_x + O(h^3). \tag{3.5}$$

The flux of the equivalent equation is also conservative for the entropy $u^2/2$, so that

$$\left(\frac{u^2}{2}\right)_t + \frac{3}{4}\big(u^4\big)_x = \frac{h\beta}{4}(u^2)_{xx} - \frac{h\beta}{2}(u_x)^2 + \frac{h^2\gamma}{3}\big(uu_{xx} - (u_x)^2/2\big)_x$$
$$- \frac{h^2}{4}\big(2\,u^3u_{xx} + u^2(u_x)^2\big)_x, \tag{3.6}$$

where the only dissipation comes from the second term on the right. Thus the equivalent equation (3.5) (with $O(h^3)$ replaced by 0) *dissipates the entropy* $u^2/2$. Once again, in (3.5), there appears to be a competition between linear and nonlinear terms in producing a sign for the dispersion.

Scheme III. Fourth-order flux:

$$g^0_{j+1/2} = \frac{1}{12}\big(-(u_{j+2})^3 + 7\,(u_{j+1})^3 + 7\,(u_j)^3 - (u_{j-1})^3\big), \tag{3.7}$$

so that

$$\frac{g_{j+1/2} - g_{j-1/2}}{h} = (u^3)_x + O(h^4).$$

The equivalent equation is

$$u_t + (u^3)_x = \frac{h\beta}{2}u_{xx} + \frac{h^2\gamma}{3}u_{xxx} + O(h^3), \tag{3.8}$$

where the third-order contribution comes from the β term in (3.1).

To second order, (3.8) (with $O(h^3)$ replaced by 0) coincides exactly with the continuous model (2.28), provided we identify $\epsilon = h\beta/2$ and $\alpha = 4\gamma/(3\beta^2)$. Equivalently, one has

$$\beta = 2\,\frac{\epsilon}{h}, \qquad \gamma = 3\,\alpha\,\left(\frac{\epsilon}{h}\right)^2. \tag{3.9}$$

In particular, the equivalent equation (3.8) is *entropy dissipative.*

Typical solutions to the Riemann problem for each of the three schemes are presented in Figure 3.1a–b. In both figures, $\beta = 10$, while in Figure 3.1a, $\gamma = 18.75$, and in Figure 3.1b, $\gamma = 75$. For both figures $u_l = 4$ and $u_r = -5$. While Scheme II produces some palpable oscillations in Figure 3.1a, it is striking that even for moderately strong shocks there are few oscillations to betray the fact that these schemes do not converge to the classical (Oleinik) solutions. Of course the presence of the intermediate state stands in contrast to the classical case.

We now discuss some heuristic arguments on excluding nonclassical shocks.

Motivated by the fact that the sign of the dispersive term is crucial to the continuous model (2.28), we now examine the equivalent equations of the three numerical schemes. In a pedestrian manner, we enforce this sign requirement, combined with information regarding the traveling wave (TW) solution of (2.28), in order to obtain a condition on γ, for fixed ϵ/h, such that the shocks will only be classical.

For weak shocks, we expect that the nonlinear contributions to the dispersion (from truncation error in the flux) will be small compared to the linear portions. This would produce discrete shocks very close to the TW solutions associated with (2.28). In particular, the TW solution of the continuous model (2.28) is known to have a "nucleation criterion," that is, a value u_{nucl} such that for a positive left state u_l less

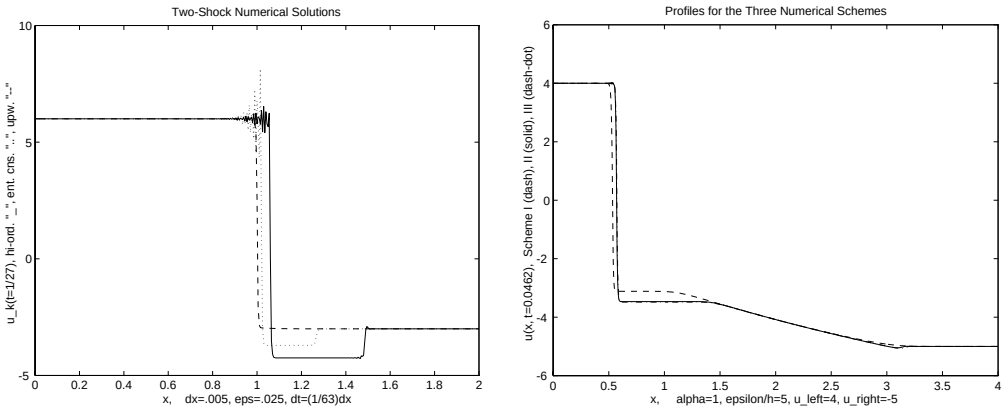

(a) **(b)**

FIG. 3.1. (a) *Two-shock solutions for Schemes* II *and* III *with* $\gamma = 18.7$*;* (b) *Nonclassical shocks and rarefactions for* $\gamma = 75$.

than u_{nucl}, there are only classical solutions (see [15, 10]). In terms of the parameter α, this value is

$$u_{nucl} = \frac{2\sqrt{2}}{3\sqrt{\alpha}}. \tag{3.10}$$

We turn first to Scheme I and its equivalent equation (3.3). The dispersive term has the form

$$C\left(2\,\gamma\,u - u^3\right)_{xxx},$$

and if we make the crude assessment that the dispersive term will have the correct sign when the quantity inside the parentheses is positive, then we need $2\gamma > u^2$, so that in order to prevent any nonclassical behavior in the numerical scheme, we need only have $u_{nucl} > \sqrt{2\gamma}$. In terms of the parameters α and γ,

$$\frac{2\sqrt{2}}{3} > \alpha\,\frac{\epsilon}{h}, \qquad \text{or} \qquad \gamma < 2\sqrt{2}\,\frac{\epsilon}{h}. \tag{3.11}$$

Fixing ϵ/h then gives an upper bound, α_{crit}, on when the solutions will be entirely classical. In section 4, we test this value with numerical experiments.

In the case of the equivalent equation (3.5) for the entropy conservative flux, it is no longer possible to write the dispersive term as $g(u)_{xxx}$, and hence to apply the idea from Scheme I above. Scheme II should also have a (lower) cut-off value for γ. It will be computed numerically in the next section.

Finally, for the high-order flux Scheme III, it appears that the numerical behavior of the scheme (based on its equivalent equation (3.8)) should mimic the solution of (2.28) for small u, regardless of the size of γ. When u is large, the equivalent equation no longer provides an accurate picture of the numerical solution.

3.2. Elastodynamics model. We now compute the equivalent equations for three choices of numerical flux in the elastodynamics model (2.17)–(2.18). We utilize

continuous in time, discrete in space approximations of the form (2.22),

(3.12)
$$\frac{dv_j}{dt} + \frac{1}{h}\,(g^{v,0}_{j+1/2} - g^{v,0}_{j-1/2}) = \frac{\beta}{h}(v_{j+1} - 2v_j + v_{j-1}) - \frac{\gamma}{h}(w_{j+2} - 2w_{j+1} + 2w_{j-1} - w_{j-2}),$$
$$\frac{dw_j}{dt} + \frac{1}{h}\,(g^{w,0}_{j+1/2} - g^{w,0}_{j-1/2}) = 0,$$

where $\beta, \gamma > 0$ are constants and h is the mesh size. The fluxes $g^{v,0}_{j+1/2}$ and $g^{w,0}_{j+1/2}$ in all three schemes are given now.

Scheme I. Lax–Friedrichs scheme:

$$\begin{aligned} g^{v,0}_{j+1/2} &= -(1/2)\big(\sigma(w_{j+1}) + \sigma(w_j)\big) - (2\lambda)^{-1}(v_j - v_{j+1}),\\ g^{w,0}_{j+1/2} &= -(1/2)(v_{j+1} + v_j) - (2\lambda)^{-1}(w_j - w_{j+1}), \end{aligned} \tag{3.13}$$

where $\sigma(w_j) := w_j^3 + a\,w_j$, for $a > 0$, and where λ is a fixed parameter. In particular, for the Riemann problem—our primary interest here—with initial data (v_l, w_l) and (v_r, w_r), we define the constant w_0 by

$$w_0^2 = \max\ (4w_l^2, 4w_r^2),$$

and set $\lambda := 3/(4\sqrt{3\,w_0^2 + a})$, in analogy with the corresponding term from the discrete Lax–Friedrichs scheme. See the discussion of the timestep in Section 4.2 for more details.

The equivalent equation is

$$\begin{aligned} &v_t - \big(\sigma(w)\big)_x = h\,\big(\beta + (2/3)\,c(w_0)\big)v_{xx} - (h^2/6)\,\big((12\gamma - a)w - w^3\big)_{xxx} + O(h^3),\\ &w_t - v_x = h\,(2/3)c(w_0)\,w_{xx} + (h^2/6)\,v_{xxx} + O(h^3), \end{aligned} \tag{3.14}$$

where $c(w_0) := \sqrt{3\,w_0^2 + a}$.

Scheme II. Entropy conservative scheme:

$$\begin{aligned} g^{v,0}_{j+1/2} &= -\big(\sigma(w_{j+1}) + \sigma(w_j)\big)/2,\\ g^{w,0}_{j+1/2} &= -(v_{j+1} + v_j)/2. \end{aligned} \tag{3.15}$$

With this choice, and for $\beta = \gamma = 0$, the scheme is entropy conservative:

$$\frac{d}{dt}\Big(\frac{v_j^2}{2} + \frac{w_j^4}{4} + \frac{a\,w_j^2}{2}\Big) + \frac{1}{h}\big(G_{j+1/2} - G_{j-1/2}\big) = 0,$$

with $G_{j+1/2} := -v_j\,w_{j+1}^3 - v_{j+1}\,w_j^3$. For arbitrary β and γ, the equivalent equation is

$$\begin{aligned} v_t - \big(\sigma(w)\big)_x &= h\,\beta\,v_{xx} - (h^2/6)\,\big((12\,\gamma - a)w - w^3\big)_{xxx} + O(h^3),\\ w_t - v_x &= (h^2/6)\,v_{xxx} + O(h^4). \end{aligned} \tag{3.16}$$

Note that the third-derivative terms from the flux both act counter to the capillarity due to γ.

Scheme III. Fourth-order flux:

$$\begin{aligned} g^{v,0}_{j+1/2}(v,w) &= -\big(-\sigma(w_{j+2}) + 7\,\sigma(w_{j+1}) + 7\,\sigma(w_j) - \sigma(w_{j-1})\big)/12,\\ g^{w,0}_{j+1/2}(v,w) &= -\big(-v_{j+2} + 7\,v_{j+1} + 7\,v_j - v_{j-1}\big)/12. \end{aligned} \tag{3.17}$$

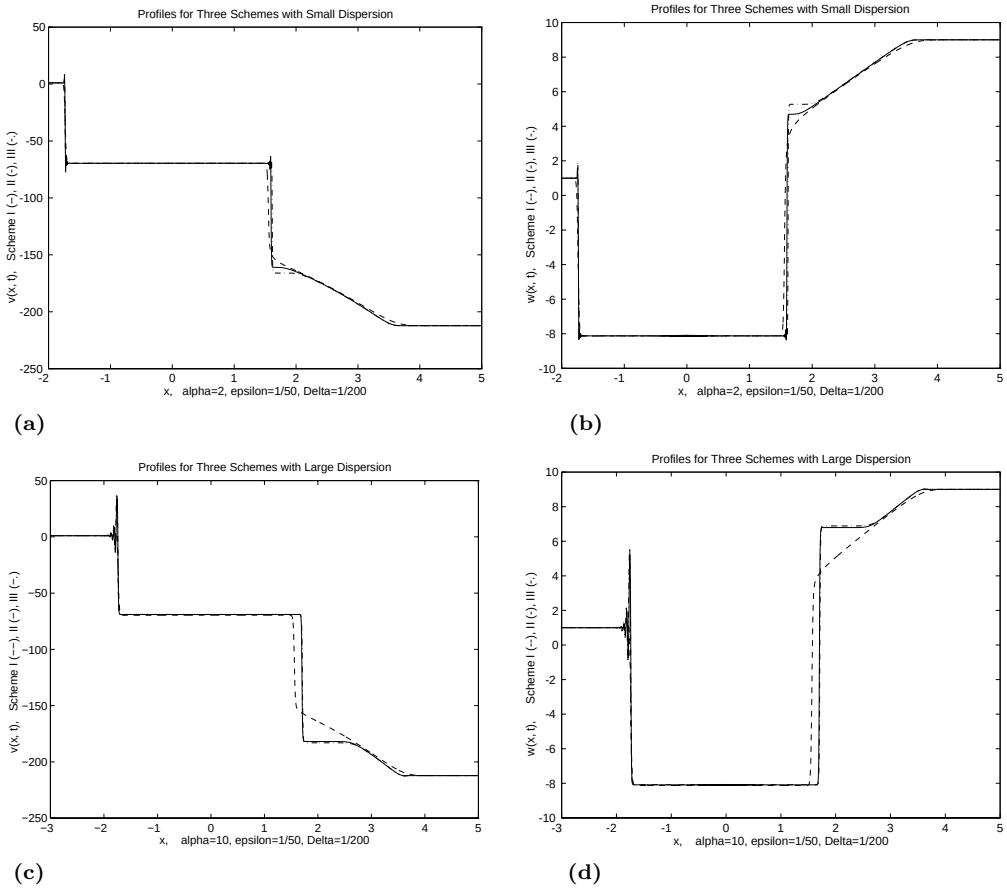

FIG. 3.2. (a) *v-component for* $\alpha = 2$*;* (b) *w-component for* $\alpha = 2$*;* (c) *v-component for* $\alpha = 10$*;* (d) *w-component for* $\alpha = 10$.

The equivalent equation is

$$\begin{aligned} v_t - \sigma(w)_x &= \beta\, h\, v_{xx} - 2\,\gamma h^2\, w_{xxx} + O(h^3), \\ w_t - v_x &= O(h^4), \end{aligned} \tag{3.18}$$

which agrees with (2.17) to $O(h^3)$, provided we identify $\epsilon = h\beta$, $\alpha = 2\,\gamma/\beta^2$. In other words, if

$$\beta = \frac{\epsilon}{h} \qquad \text{and} \qquad \gamma = \frac{\alpha}{2}\left(\frac{\epsilon}{h}\right)^2. \tag{3.19}$$

Finally we present some heuristic arguments for a threshold of nonclassical behavior.

In the equivalent equation (3.16) for the entropy conservative flux (Scheme II), the sign of the capillarity term,

$$C\,(12\,\gamma w - a\,w - w^3)_{xxx},$$

can now change, depending upon a balance between linear and nonlinear effects. As a minimal requirement, it appears that one needs $\gamma > a/12$, in order to observe

nonclassical behavior. Preliminary information concerning traveling wave solutions of (2.17) [26] indicates that like the scalar equation, there is a nucleation criterion for the system. If we denote by w_{nucl} the value below which all TW solutions of (2.17) converge strongly to classical shocks—note that w_{nucl} will be a function of γ and ϵ/h—then we have the following algebraic condition: In order to exclude n.c. shocks from Scheme II, one must have

$$\gamma < (a + w_{nucl}^2)/12. \tag{3.20}$$

Taking $a = 1$, we now plot typical profiles in both v and w for Schemes I–III for both small and large values of γ. In Figure 3.2a, we plot the v-component when $\alpha = 2$, with the w-component graphed in Figure 3.2b. Then in Figure 3.2c, we take $\alpha = 10$ and plot the v-component, while the w-component for this α is drawn in Figure 3.2d. While the left-moving shock is always classical, with $w_r < -2w_l$, the right-moving shocks are nonclassical in the case Schemes II and III, with the intermediate state and the separation in wavespeed more pronounced in Figures 3.2c and 3.2d. The oscillations appear almost exclusively in the left-moving, classical shock.

4. Kinetic relation. We now study numerically nonclassical shocks for the schemes introduced in section 3. In comparing the continuous and discrete models, we emphasize that for small or even moderate-size shocks the entirety of nonclassical shocks for both continuous and discrete models are quite close together. This is measured by drawing the kinetic function in the state variables, i.e., the right-hand state of nonclassical shock as a function of its left-hand state. From this we calculate the kinetic function, providing the entropy dissipation across a shock as a function of its propagation speed.

The kinetic relation depends not only on the parameter α in the continuous model, but on both the ratios of β/γ and ϵ/h in the numerical schemes.

4.1. Cubic conservation law. The first set of figures pertains to Schemes I, II, and III for the cubic scalar equation (2.26). In Figures 4.1a and 4.1b we plot the intermediate/right-hand state, u_m, of the Riemann solution versus the left-hand state, u_l, as this latter quantity is varied from 0 to 16.5 in increments of 0.15. In each of the runs, the Riemann data chosen were

$$u_j(0) = \begin{cases} u_l, & j \le 0, \\ u_r = -1.25\, u_l, & j > 0. \end{cases} \tag{4.1}$$

For initial data (4.1), the Riemann solution consists of a shock from u_l to $u_m \in [-u_l, -u_l/2]$, followed by a smooth rarefaction from u_m to u_r. When the kinetics select the classical solution, $u_m = -u_l/2$. This upper boundary is drawn with a dashed line in Figures 4.1a and 4.1b. The "most" nonclassical solution, with $u_m = -u_l$, is also drawn with a dashed line.

With the above Riemann data, the shock corresponding to the TW solution of the continuous model (2.28) (see [15, 10]) takes the form

$$u_m = \begin{cases} -\frac{u_l}{2}, & 0 \le u_l \le \frac{2\sqrt{2}}{3\sqrt{\alpha}}, \\ -u_l + \frac{\sqrt{2}}{3\sqrt{\alpha}}, & u_l > \frac{2\sqrt{2}}{3\sqrt{\alpha}}, \end{cases} \tag{4.2}$$

where $\alpha\,\epsilon^2$ multiplies the dispersive term in (2.28); that is, the shock remains classical until u_l is sufficiently large, compared with $1/\sqrt{\alpha}$. Beyond this point, the TW solution

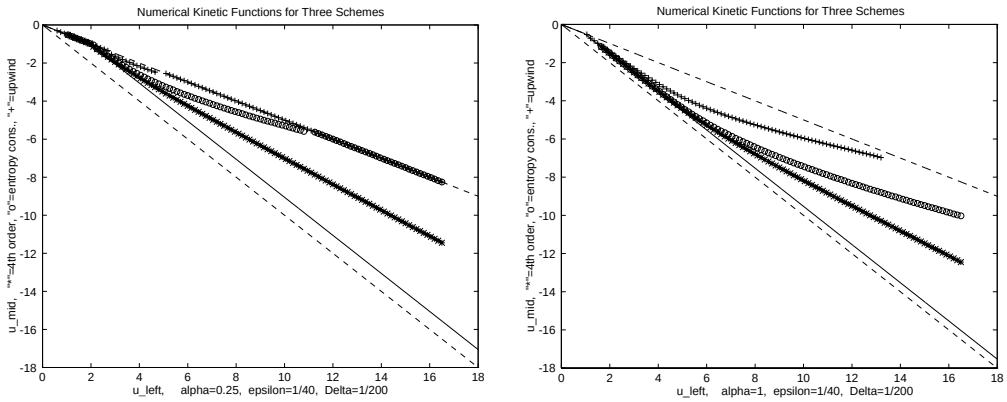

(a) **(b)**

FIG. 4.1. (a) $\alpha = 0.25$; (b) $\alpha = 1.0$.

is nonclassical, differing from $-u_l$ by a constant. This TW solution, (4.2), is plotted with a solid line in Figures 4.1a and 4.1b.

In Figures 4.1a and 4.1b, we chose mesh spacing $h = 1/200$ and diffusion $\epsilon = 1/40$ and used fourth-order Runge–Kutta for time stepping. The CFL number was taken to be as large as possible in each run (each of the three curves contains approximately 100 such runs) and was identical for both the entropy conservative and fourth-order flux models. A slightly smaller time-step was required for the upwinding scheme. In Figure 4.1a we took $\alpha = 1$, while in Figure 4.1b we chose $\alpha = 0.25$.

As might be expected, the larger value of α in Figure 4.1b gives rise to a "more nonclassical" kinetic function; i.e., the curves stay farther away from the classical (upper dashed) line. From most nonclassical to most classical, in both plots, were the fourth-order scheme, the entropy conservative scheme, and the upwinding scheme, respectively. The fourth-order flux scheme also stays closest to the TW solution of (2.28) for the widest range of u_l. This is not surprising, as the equivalent equation for the fourth-order flux scheme most closely approximates (2.28). Notice that in no case are the right-hand states more nonclassical than the traveling wave solution.

In Figures 4.1c and 4.1d, we plot the numerical kinetic functions in the state variables using the data on left- and right-hand states from Figures 4.1a and 4.1b, respectively. We use the quadratic entropy $U(u) = u^2/2$ in computing the entropy dissipation. In terms of u_l and u_m, this is

$$\phi(u_l, u_m) = (u_m - u_l)^2(u_m^2 - u_l^2)/4. \tag{4.3}$$

From the Rankine–Hugoniot relation, the shock speed is

$$s = u_l^2 + u_l u_m + u_m^2, \tag{4.4}$$

and formulas (4.3)–(4.4) provide a parametric representation of the kinetic function $\varphi(s)$. (Cf. [10].) In Figure 4.1c, all numerical kinetic functions lie close to the classical kinetic function, with Scheme I closer than II, which is, in turn, closer than III. In Figure 4.1d, both Schemes II and III begin along the TW kinetic function but gradually transition to classical kinetics.

In section 3, we gave some heuristic criteria to decide whether for a given numerical scheme, and a fixed set of parameters, the shocks would be entirely classical.

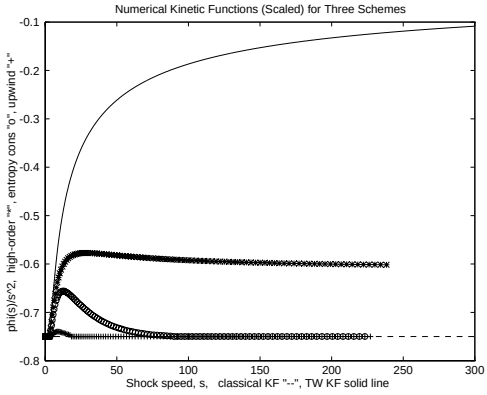

(c)

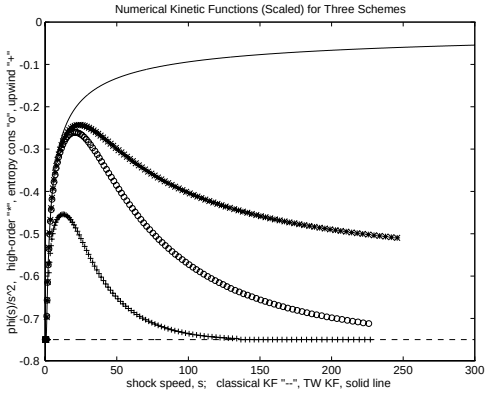

(d)

FIG. 4.1. (*cont.*). *Scaled entropy dissipation,* $\phi(s)/s^2$, *vs. shock speed,* s, *for three numerical schemes.* (c) $\alpha = 0.25$, (d) $\alpha = 1.0$.

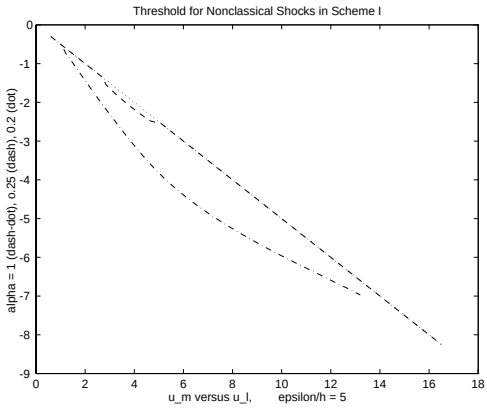

(e)

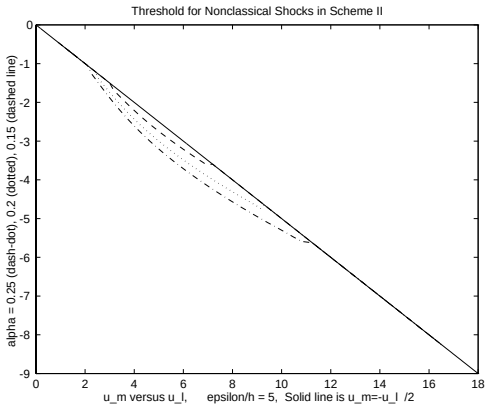

(f)

FIG. 4.1. (*cont.*). (e) *Scheme* I *has n.c. threshold* $0.2 < \alpha < 0.25$. (f) *Scheme* II *has n.c. threshold* $0.1 < \alpha < 0.15$.

We now test these criteria for the three schemes. In Figure 4.1e, we plot the left- and right-hand states of the shocks for the upwinding scheme. We took $\epsilon/h = 5$, so that $\gamma = 75\alpha$, and several values of α: $0.25, 0.2$, and 0.15. From condition (3.12), we estimate the cut-off value of α to be $\alpha_{crit} = 0.19$ and, indeed, we observe experimentally that the cut-off occurs in the range $0.2 < \alpha < 0.25$. For $\alpha = 0.25$, the curve dips below the classical, $u_m = -u_l/2$-line, while it never deviates from this line when $\alpha \leq 0.2$.

For the entropy conservative flux (Scheme II), we again take $\epsilon/h = 5$, and now take $\alpha = 0.25, 0.2, 0.15$, and 0.1. These data are plotted in Figure 4.1f. Similar phenomena occur, only now at smaller values of α: the cut-off occurs for $0.1 < \alpha < 0.15$.

Focusing next on the fourth-order flux scheme, we first plot the right- vs. left-hand states for small α: 0.2, 0.1, and 0.0. This is depicted in Figure 4.1g. Notice that even when $\alpha = 0$, the solution to Scheme III is classical, as would be predicted by the equivalent equation, out to $u_l \leq 6$. For stronger shocks, the equivalent equation fails to predict the right-hand state of the scheme. Indeed the kinetic function appears to

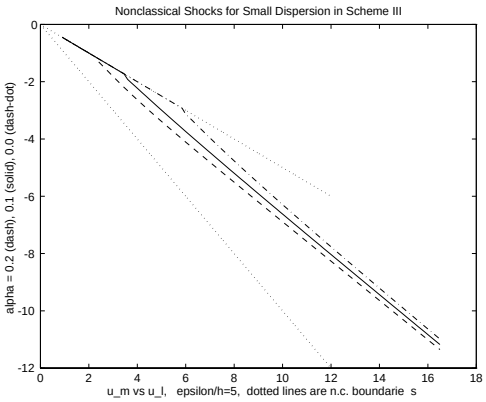

(g)

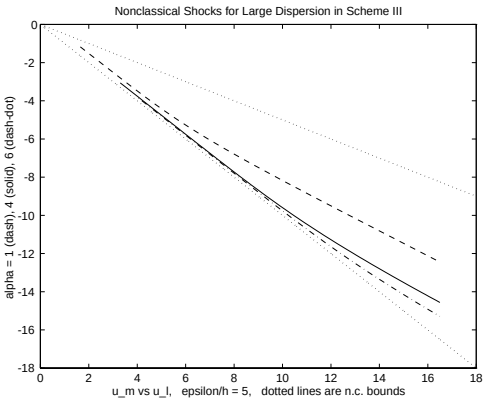

(h)

FIG. 4.1. (*cont.*). (g) *For small* α, *Scheme* III *gives neither the classical nor the TW solution to* (2.28). (h) *For large* α, *Scheme* III *gives the solution of* (2.28).

have a distinct limit as $u_l \to \infty$.

When we take α (i.e., γ) large in Scheme III, which is in some sense what we should do in order to dominate higher-order terms, then the solution approaches the limiting TW solution of (2.28). This can be seen in Figure 4.1h.

4.2. Elastodynamics model. We now turn to the elastodynamics model and the numerical kinetic relations for Schemes I, II, and III. Once again we determine the kinetic function in the state variables by plotting the left- and right-hand states of a shock (in this case, the w-component of the 2-shock) for a range of left-hand states. For Riemann data in Schemes I and II, we took

$$\big(v_k(0), w_k(0)\big) = \begin{cases} (1,1), & k \le 0, \\ (v_r, w_r), & k > 0. \end{cases} \tag{4.5}$$

The value of w_r is increased from 0 to approximately 22, in increments of 0.2. For each of these runs, v_r is selected to lie well within the region of the (v,w)-plane which, depending on the viscosity and capillarity, gives rise to nonclassical shocks; i.e., the Riemann solution must twice cross the v-axis. Specifically, if $(v_*, 0)$ lies on the 1-wave integral curve from (v_l, w_l), then $v_* = v_l - F_l + F_0$, where $F_l = \sqrt{3/4}\,\big(w_l c_l + (1/3)\log(w_l + c_l)\big)$, $c_l = \sqrt{w_l^2 + 1/3}$, and $F_0 = .5 - (1/\sqrt{48})\log 3$. We then chose v_r to lie well below the 2-wave integral curve from $(v_*, 0)$: $v_r = v_* - 3(F_r - F_0)$, where $F_r = \sqrt{3/4}\big(w_r c_r + (1/3)\log(w_r + c_r)\big)$ and $c_r = \sqrt{w_r^2 + 1/3}$. Here we have used $a = 1$.

The above choice of (v_l, w_l) and (v_r, w_r) induces a 1-wave fan (including either a classical or nonclassical shock) from (v_l, w_l) to a point (v_m, w_m). For purposes of computing the numerical kinetic function, $w_m < 0$ is taken as the left-hand state of the shock. Owing to our choice of (v_r, w_r), with $w_r > 0$, the state (v_m, w_m) is connected by a 2-shock to (v_{i_2}, w_{i_2}); this shock may either be classical, with $w_{i_2} = -w_m/2$, or nonclassical, with $w_{i_2} \in [-w_m, -w_m/2)$.

In Figures 4.2a and 4.2b we chose a gridsize of $h = 1/400$, with the viscosity fixed at $\epsilon = 1/100$. For all three schemes, we used fourth-order Runge–Kutta for time stepping with the condition $\lambda = 0.75/\sqrt{3\,w_0^2 + a}$, where $w_0^2 = \max(4w_l^2, 4w_r^2)$ is an upper bound on $\|w\|_{\mathbf{L}^\infty}^2$, coming from the fact that for classical shock-rarefaction in the 2-wave family, $w_m = -2w_{i_2}$, and $w_r \ge w_{i_2}$, with equality only when the rarefaction

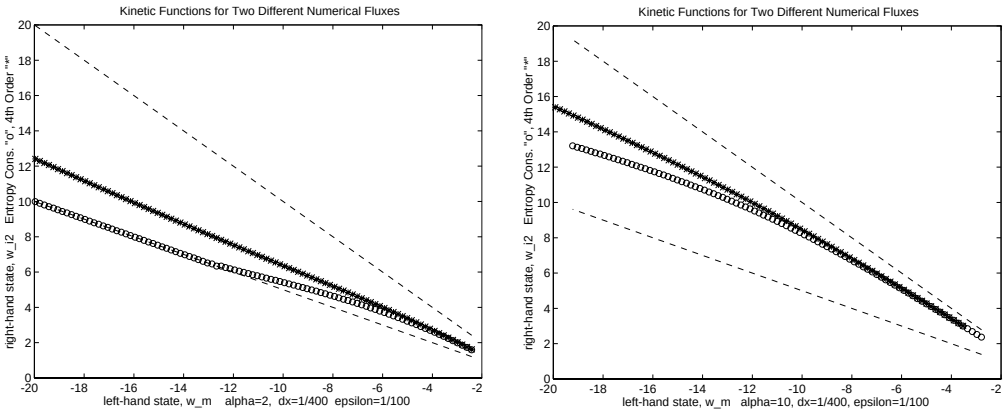

(a) **(b)**

FIG. 4.2. (a) $\alpha = 2$, *the data for Scheme* I *is not drawn in but follows precisely the lower, dashed line.* (b) $\alpha = 10$. *Again, Scheme* I *shocks are entirely classical and are not drawn in.*

is degenerate. Time steps were identical for corresponding runs of each scheme.

Besides the data points from the various runs, the boundaries for possible classical and nonclassical shocks are plotted (dashed lines) in Figures 4.2a and 4.2b. The lower line, $w_{i_2} = -w_m/2$, represents a kinetic function which always selects the classical solution, while the upper dashed line, $w_{i_2} = -w_m$, corresponds to the "most" nonclassical kinetic function.

In Figure 4.2a, we took $\alpha = 2$, while in Figure 4.2b, $\alpha = 10$. In both cases, Scheme I gives only classical behavior. Consequently, the data from Scheme I is excluded from Figures 4.2a and 4.2b in order to clarify the presentation. Notice that in Figure 4.2a, the Scheme II shocks return to the classical line, for $w_m \geq 12$, while those of Scheme III continue along an n.c. trajectory. Then in Figure 4.2b, the curves for Schemes II and III have a region of overlap, but Scheme II ultimately arcs back toward the classical solutions. In all curves, note that w_{i_2} is monotone decreasing with w_m.

In Figures 4.2c and 4.2d, we plot the numerical kinetic functions, based on the left- and right-hand states in Figures 4.2a and 4.2b, respectively, and using the entropy (2.19). The entropy dissipation is

$$\phi(w_-; w_+) = (w_+^2 + w_+ w_- + w_-^2 + a)^{1/2}(w_+ - w_-)^3(w_+ + w_-)/4. \tag{4.6}$$

In Figure 4.2c, the kinetics for Schemes I and II are nearly identical (classical) for $s \geq 6$. In Figure 4.2d, all three kinetic functions are quite distinct at large values of s.

We now turn to small values of the dispersion and to the existence of threshold values in γ for the existence of n.c. shocks. In Figure 4.2e, it can be seen that the behavior of Scheme I is always classical, except for very large dispersion, $\alpha = 40$, i.e., $\gamma = 320$. This latter, rather jagged curve should only be taken as an indication of n.c. behavior in Scheme I; the nonmonotonicity of this curve is inconsistent with other numerical experiments of this type. In Figure 4.2f, we plot the left- vs. right-hand states for Scheme II, with several choices for α : 2.0, 1.0, 0.5, and 0.25. The last two choices both return purely classical behavior, while $\alpha = 1$ has only a tiny interval in w_m for n.c. shocks. The numerical threshold for Scheme II to produce n.c. shocks is therefore $4 < \gamma < 8$.

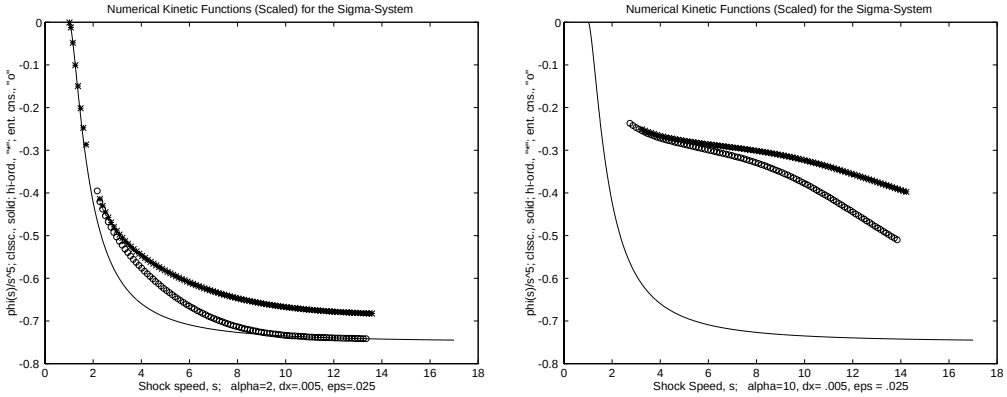

(c) **(d)**

FIG. 4.2. (*cont.*). *Scaled entropy dissipation,* $\phi(s)/s^5$, *vs. shock speed,* s, *for Schemes* II *and* III. *Scheme* I *gives the classical, solid curve.* (c) $\alpha = 2$; (d) $\alpha = 10$.

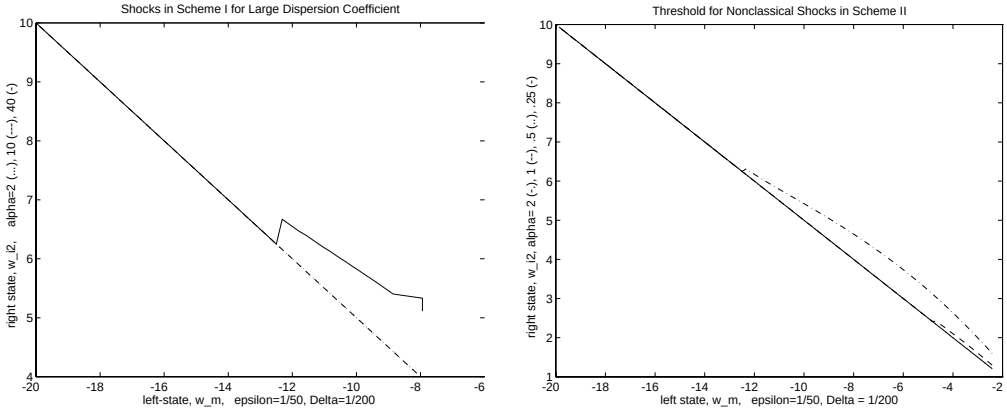

(e) **(f)**

FIG. 4.2. (*cont.*). (e) *Classical and (likely) n.c. behavior for large* α *in Scheme* I. (f) *Threshold for n.c. shocks in Scheme* II *is* $.5 < \alpha < 1$.

For Scheme III, we consider the behavior both for γ small (Figure 4.2g) and γ large, (Figure 4.2h). Note that in Figure 4.2b, the curves approach the classical line, and that when $\alpha = 0.5$, the solution is, in fact, classical out to $w_m = 12$, at which point it gives rise to n.c. shocks. Similar behavior occurs when $\alpha = 0$, but now the transition occurs at a larger value, $w_m = 16.5$.

At the other end of the spectrum, for large γ, the curves in Figure 4.2h straighten out and parallel the maximally n.c. curve, where $w_{i_2} = -w_m$. It will be interesting to compare the curves in this large α limit with n.c. traveling wave solutions to the elastodynamics model.

5. Concluding remarks. We have shown that schemes balancing diffusion and dispersion may generate nonclassical shock waves which do not satisfy the Liu criterion. To characterize these new shocks, we introduced the kinetic function, expressed either in the state variables or—when possible—parametrized by shock speed. It was shown to be an efficient tool to study sensitive dependence on the ratios of diffu-

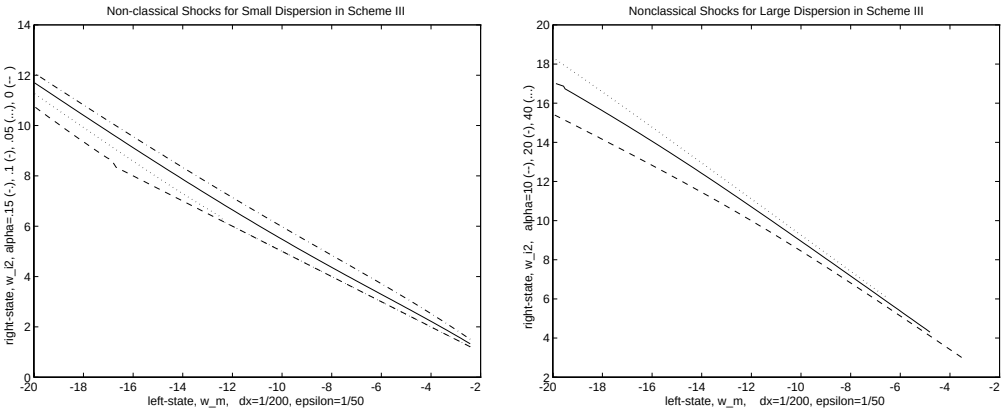

(g) **(h)**

FIG. 4.2. (*cont.*). (g) *Small* α *in Scheme* III*;* (h) *large* α *in Scheme* III.

sion/dispersion, diffusion/mesh size, the order of accuracy of the discretization, etc. Our study sheds light on the design of numerical schemes for problems containing small-scale dependent shock waves.

One requirement is to ensure that the scheme is consistent with the natural entropy induced by the continuous model,

$$U(u)_t + F(u)_x \leq 0. \tag{5.1}$$

By itself, (5.1) does not guarantee uniqueness (say, for the Riemann problem) but does severely restrict the class of admissible solutions. The analysis in [11] shows that at most one parameter per wave family is left undetermined. In view of our numerical experiments, we expect that for most practical applications the corresponding parameters occupy a *very limited range.* It would be interesting to characterize this range for specific physical applications, such as the dynamics of austenite-martensite phase transformations in solids, or the magnetohydrodynamics of the solar wind past earth's magnetosphere.

We find that numerical schemes whose equivalent equations best mimic the continuous model provide better approximations than either first-order or entropy conservative schemes. Still, for shocks with large strength, numerical solutions diverge from those of the continuous model. In fact, we show that the ϵ-limit of the solutions to the continuous model differ from the continuum limit of the numerical solutions u^h as the mesh is refined:

$$\lim_{\epsilon \to 0} u^\epsilon \neq \lim_{h \to 0} u^h. \tag{5.2}$$

For small shock strength, this discrepancy is so subtle that it is often difficult to detect. Moreover the continuous model may not have this degree of accuracy. In fact, many are derived using assumptions of the magnitude of the relevant variables and with experimental tolerances in the coefficients and data. The results presented here justify that for many practical purposes, one may use the discrete model as a good approximation to the continuous one. Indeed, it may be very difficult in practice to determine the small-scale effects in the continuous model accurately, the experimental data being out of reach for various reasons.

When one is interested in large-time calculations, however, there is a real possibility that the error between the continuous and the discrete models will accumulate and that the corresponding solutions will eventually differ substantially. For strong shocks, the same effect may occur.

The generalization of this work to physical models from phase dynamics [12] is currently in progress.

Acknowledgment. The authors are grateful to Eitan Tadmor for pointing out the relevance of [30].

REFERENCES

[1] R. Abeyaratne and J. K. Knowles, *Kinetic relations and the propagation of phase boundaries in solids*, Arch. Rational Mech. Anal., 114 (1991), pp. 119–154.

[2] R. Abeyaratne and J. K. Knowles, *Implications of viscosity and strain gradient effects for the kinetics of propagating phase boundaries in solids*, SIAM J. Appl. Math., 51 (1991), pp. 1205–1221.

[3] M. Affouf and R. Caflisch, *A numerical study of Riemann problem solutions and stability for a system of viscous conservation laws of mixed type*, SIAM J. Appl. Math., 51 (1991), pp. 605–634.

[4] D. Amadori, P. Baiti, P. G. LeFloch, and B. Piccoli, *Nonclassical shocks and the Cauchy problem for nonconvex conservation laws*, J. Differential Equations, to appear.

[5] B. Cockburn and H. Gau, *A model numerical scheme for the propagation of phase transitions in solids*, SIAM J. Sci. Comput., 17 (1996), pp. 1092–1121.

[6] J. Correia and P.G. LeFloch, *Diffusive-dispersive approximations of multidimensional conservation laws*, in Nonlinear Partial Differential Equations, World Scientific Publishing, River Edge, NJ, 1998, to appear.

[7] J. Goodman and A. Majda, *The validity of the modified equation for nonlinear shock waves*, J. Comput. Phys., 58 (1985), pp. 336–348.

[8] A. Harten, *High resolution schemes for hyperbolic systems of conservation laws*, J. Comput. Phys., 49 (1983), pp. 357–393.

[9] A. Harten, J. M. Hyman, and P. D. Lax, *On finite-difference approximations and entropy conditions for shocks*, Comm. Pure Appl. Math., 29 (1976), pp. 297–322.

[10] B. T. Hayes and P. G. LeFloch, *Non-classical shocks and kinetic relations: Scalar conservation laws*, Arch. Rational Mech. Anal., 139 (1997), pp. 1–56.

[11] B. T. Hayes and P. G. LeFloch, *Non-classical shocks and kinetic relations: Hyperbolic systems*, SIAM J. Math. Anal., submitted.

[12] B. T. Hayes, P. G. LeFloch, and M. Shearer, *Non-classical shocks and kinetic relations: Systems of mixed type*, in preparation.

[13] T. Y. Hou and P. G. LeFloch, *Why non-conservative schemes converge to wrong solutions: Error analysis*, Math. Comp., 62 (1994), pp. 497–530.

[14] T. Y. Hou, P. G. LeFloch, and P. Rosakis, *Dynamics of phase interfaces: A level set approach*, in preparation.

[15] D. Jacobs, W. R. McKinney, and M. Shearer, *Traveling wave solutions of the modified Korteweg-deVries Burgers equation*, J. Differential Equations, 116 (1995), pp. 448–467.

[16] S. Jin, *Numerical integrations of systems of conservation laws of mixed type*, SIAM J. Appl. Math., 55 (1995), pp. 1536–1551.

[17] S. Karni, *Viscous shock profiles and primitive formulations*, SIAM J. Numer. Anal., 29 (1992), pp. 1591–1609.

[18] P. D. Lax, *Hyperbolic systems of conservation laws*, II, Comm. Pure Appl. Math., 10 (1957), pp. 537–566.

[19] P. D. Lax, *Hyperbolic Systems of Conservation Laws and the Mathematical Theory of Shock Waves*, SIAM, Philadelphia, 1973.

[20] P. D. Lax and B. Wendroff, *Systems of conservation laws*, Comm. Pure Appl. Math., 13 (1960), pp. 217–237.

[21] P. G. LeFloch, *Propagating phase boundaries: Formulation of the problem and existence via the Glimm scheme*, Arch. Rational Mech. Anal., 123 (1993), pp. 153–197.

[22] P. G. LeFloch and R. Natalini, *Conservation laws with vanishing nonlinear diffusion and dispersion*, Nonlinear Anal., to appear.

[23] D. Levermore, *personal communication*, 1996.

[24] T. P. Liu, *The Riemann problem for general* 2×2 *conservation laws*, Trans. Amer. Math. Soc., 199 (1974), pp. 89–112.
[25] M. E. Schonbek, *Convergence of solutions to nonlinear dispersive equations*, Comm. Partial Differential Equations, 7 (1982), pp. 959–1000.
[26] M. Shearer, *personal communication*, 1997.
[27] C. W. Shu, *A numerical method for systems of conservation laws of mixed type admitting hyperbolic flux splitting*, J. Comput. Phys. 100 (1992), pp. 424–429.
[28] M. Slemrod and J. E. Flaherty, *Numerical integration of a Riemann problem for a van der Waals fluid*, in Phase Transformations, E. C. Aifantis and J. Gittus, eds., Elsevier Applied Science Publishers, New York, 1986, pp. 203–212.
[29] E. Tadmor, *Numerical viscosity and the entropy condition for conservative difference schemes*, Math. Comp., 43 (1984), pp. 217–235.
[30] E. Tadmor, *The numerical viscosity of entropy stable schemes for systems of conservation laws*, Math. Comp., 49 (1987), pp. 91–103.
[31] L. Truskinovsky, *Dynamics of non-equilibrium phase boundaries in a heat conducting nonlinear elastic medium*, J. Appl. Math. Mech. (PMM), 51 (1987), pp. 777–784.
[32] L. Truskinovsky, *Kinks versus shocks*, in Shock Induced Transitions and Phase Structures in General Media, IMA Vol. Math. Appl. 52, R. Fosdick, E. Dunn, and H. Slemrod, eds., Springer-Verlag, New York, 1993.
[33] X. Zhong, T. Y. Hou, and P. G. LeFloch, *Computational methods for propagating phase boundaries*, J. Comput. Phys., 124 (1996), pp. 192–216.